ANALYSIS OF LOW CYCLE FATIGUE PERFORMANCE OF WELDED STRUCTURAL JOINTS

O. LOMACKY, B. ELLINGWOOD, L.N. GIFFORD

Department of the Navy,
Naval Ship Research and Development Center, Bethesda, Maryland 20084, U.S.A.

SUMMARY

The current and projected use of high strength materials for pressure vessels requires that increased attention be directed toward their low-cycle fatigue performance characteristics at the design stage, as existing data show conclusively that an increase in material strength does not result in a corresponding increase in resistance to fatigue.

Welded joints are particularly fatigue-sensitive because of stress concentrations and residual stresses. To minimize and control the fatigue problem in design and to identify potential trouble spots in existing structures, a fatigue analysis methodology is being developed which systematically accounts for the major factors affecting cycle-induced fatigue response and from which predictions of both fatigue crack initiation and stable crack growth can be made.

Parameters in this analytical model are obtained from testing small specimens under rigidly controlled conditions. These include the determination of cyclic stress-strain curves, base line crack initiation data and crack growth rates. Finite element methods employing specialized elements at the crack site are used to determine the stress concentration and stress intensity factors at the fatigue-critical locations in the welded structural detail. Subsequent predictions of performance in large weldments can then be made using small specimens fatigue data in a consistent analytical framework. Because of the random nature of certain aspects of the fatigue problem, it is necessary that certain portions of the above analytical methodology be treated probabilistically.

The paper contains a synopsis of above concepts and an illustration of their application to the fatigue analysis of a butt welded joint.

1. Introduction

Welded joints are particularly sensitive to low-cycle fatigue on account of stress concentrations at abrupt changes of weld geometry, initial flaws and detrimental residual stresses resulting from the fabrication processes. Consequently, efficient utilization of high strength materials with the attendant increase of design stresses requires that increased attention be directed toward low-cycle fatigue performance. The problem is accentuated by the fact that, for many of these materials, increase in static strength is not accompanied by improved fatigue properties. Clearly, improved fatigue analysis and design methodology would prove cost effective for several reasons. First, it would afford a systematic means for selecting most appropriate material for a particular structural application by anticipating and thus minimizing and controlling fatigue problems at the design planning stage. Second, it would lead to better estimates of lifetime structural reliability and provide a rational basis for the formulation of surveillance and maintenance policies.

In a gross structural sense, the mechanism causing fatigue crack initiation and growth is highly localized, depending primarily on the stress-strain behavior at sites where crack initiation and subsequent growth occur; these sites can be identified with the location of structural discontinuities such as notches and cracks at the weld joints. Once this behavior is determined, fatigue response of complex structural details can be predicted with the aid of statistical concepts from the characteristics of the small laboratory baseline data. Such data is obtained in the environment, stress-strain state and cycling conditions approximating the service conditions at fatigue critical locations.

There are three major aspects of this work. The first is concerned with the analytical models for initiation and crack growth, respectively, under idealized conditions where all significant variables are assumed to be deterministic (single valued). These variables include the load spectrum, residual stresses, notch acuity and/or initial crack sizes, as well as the data from material characterization tests which include stress-strain curves (static and cyclic), crack initiation and crack growth rate information.

The second is concerned with the development of computer based finite element methods appropriate for the analysis of stress and deformation fields at structural discontinuities. The results are used in the formulation of analytical models discussed above in cases where the accuracy of approximate stress analysis formulas has not been established. A case in point is the calculation of stress concentration and stress intensity factors in the regions of high stress gradients.

The third is based on the extension of the above work to the formulation of mechanical probabilistic models and the development of computer-based reliability analysis. Here, the aim is to provide a transition between the deterministic models of fatigue and fracture and the service conditions where many of the critical parameters can be described only in a probabilistic sense.

This paper outlines the developments of fatigue analysis procedures along the lines discussed above. At the end, an example of the application of the concepts is illustrated by means of an example.

2. Crack Initiation Analysis

2.1 General Considerations

Cracks which initiate in pressure vessels due to fatigue cycling are usually observed to occur at stress concentrations in welds, e.g., the geometrical notch that arises from weld undercutting. Although the net section (nominal) stress usually remains elastic, the stress raiser causes a small volume of material to undergo reversals of plastic deformation; this leads to the initiation of cracks in something less than 100,000 cycles, the so-called low-cycle fatigue regime. The actual number of cycles required for initiation depends on the nominal stress range, the severity of the stress concentration and the manner in which the metal responds to inelastic cycling.

With the advent of fracture mechanics there is a tendency to neglect crack initiation phase and start the fatigue analysis assuming pre-existing flaws. Although it may be argued that consideration of propagation alone is conservative this philosophy fails to motivate improved weld detailing since it is in mitigating crack initiation that this most readily pays off. The S-N Goodman diagram approach to low cycle fatigue analysis is not considered adequate, but improved methods are now available, as discussed below.

Since crack initiation is a highly localized process, there is no reason to suspect that the cracking behavior in a large structure will differ from that of a small fatigue specimen, provided that the stress-strain conditions at the crack initiation site in the structure can be determined with reasonable accuracy and then duplicated in the specimen.

The analytical procedure for predicting crack initiation in structural weld is summarized in Figure 1 on the basis of the above assumption. Stress concentration factors are used to relate the large-scale structural information to the highly localized material response at crack sites. Calculation of stress concentration factors can be based on standard formulas or, in the case of highly complex detail geometries, by using specialized finite element methods as shall be discussed later. Predictions of crack initiation can then be made by using small specimen fatigue data in a consistent analytical framework. Key elements in the analysis are discussed below.

2.2 Material Characterization Data

This aspect can be studied with small specimen testing program. It is necessary to obtain stress-strain relations and crack initiation data from smooth specimens.

The material stress-strain relationship changes after repeated reversals of cyclic plasticity. It eventually stabilizes, however, and yields a cyclic stress-strain curve which reflects the change in the resistance of the metal resulting from cyclic deformations. The cyclic stress-strain curves are determined by using the small axial specimen shown schmetically in Figure 1. Morrow [1] has suggested that the cyclic stress-strain relation be expressed analytically by

$$\frac{\Delta\epsilon}{2} = \frac{\Delta\sigma}{2E} + \left(\frac{\Delta\sigma}{2K}\right)^{1/n} \qquad (1)$$

and which $\Delta\epsilon$ and $\Delta\sigma$ are strain and stress ranges and K and n are cyclic strength coefficient and strain hardening exponent respectively. For steel in the 80 ksi yield strength range the representative values are approximately K = 158 and n = 0.12. Dividing the stress strain ranges by factor of 2 as in eq. (1) converts into the relation between stress and strain amplitudes observed for monotonic loading of strain hardening type material. This allows a direct comparison between monotonic and cyclic stress strain curves. Note that if a cyclically stablized material is loaded monotonically the stress strain behavior will follow the cyclic and not the first excursion (monotonic) stress strain curve. For cyclic softening material the monotonic curve will be above the cyclic curve as indicated schematically in Figure 1.

It has been observed [2] that the number of cycles required to initiate fatigue cracks under low-cycle fatigue conditions depends primarily on the strain range at the crack initiation site. The baseline relationship between strain and cycles is found from regression analysis of data obtained from constant-amplitude, fully reversed (zero-mean stress and strain) strain cycling of smooth specimens. Most simply as observed by Gross [2]

$$\Delta\epsilon_T N_i^m = C \qquad (2)$$

where $\Delta\epsilon_T$= total fully reversed strain (elastic + plastic)
N_i = cycles to initiation, and m and c are material constants. Gross [2] reports that for steel in 80 ksi yield strength range m = 0.32 and c = 0.14. It has been observed that when $\Delta\epsilon_T > 0.02$, eq. (2) slightly underestimates crack initiation and thus is conservative. However, its predictive capability is excellent compared to higher order expressions at least in a statistical sense when viewed over the range of strains appropriate to the fatigue analysis of pressure vessels (say, 0.005 - 0.02).

The above relations may be established with an experimental program using either axial tension or smooth bending specimens shown schematically in Figure 1. The bending specimen is particularly suitable in that it is easily tested under fixed deflection control at relatively high strains without stability problems. The test section approximates the condition of plane strain on the surface simulating the conditions at the notch. Our criterion for crack initiation is the formation of an engineering size, readily detectable surface flaw. This corresponds roughly to the appearance of one or more flaws ranging from 1/8" to 3/16" in length. By sectioning of the specimens and statistical evaluation it was found that the initiated flaws were nearly semielliptical with a mean aspect ratio $a/_{2c}$= 0.36 where a is the flaw depth and 2c is the surface length. This information is used in crack propagation and reliability analysis.

Where a mean stress is present, its effect on crack initiation period can be determined as suggested by Smith [3] by reducing the asymmetric stress-strain hysteresis to an "equivalent" fully reversed cycle by

$$\left(\Delta\sigma_{FR}\,\Delta\epsilon_{FR}\,E\right)^{1/2} = \left(\frac{2E}{1-R}\,\Delta\sigma\,\Delta\epsilon\right)^{1/2} \quad ; \quad R = \sigma_{MIN}/\sigma_{MAX} \qquad (3)$$

Here σ_{MIN} and σ_{MAX} are respectively the maximum and minimum stress of the cycle and $\Delta\sigma_{FR}$, $\Delta\epsilon_{FR}$ are the equivalent stress and strain ranges. Subsequently using eq. (2) with $\Delta\epsilon_{FR} = \Delta\epsilon$ we make crack initiation predictions. Other factors may also affect crack initiation predictions when Equations (2) and (3) are used. These factors include prestraining, mean cycling strain and cycle-dependent mean strain creep.

2.3 Stress Analysis and Notch Sensitivity

An elastoplastic deformation analysis is required to relate the notch stress-strain response to the known nominal loading. Here, the word notch is used generically to describe stress raisers such as holes, grooves, fillets, etc. As a first order approximation a variant of the Neuber rule [4] proposed by Topper [5] is used.

$$K_f = (K_\sigma K_\epsilon)^{1/2} \tag{4}$$

in which K_σ and K_ϵ are stress and strain concentration factors and K_f is a stress-strain amplification factor for fatigue; $K_\sigma = \frac{\Delta\sigma}{\Delta S}$ and $K_\epsilon = \frac{\Delta\epsilon}{\Delta e}$ where $\Delta\sigma$, $\Delta\epsilon$ are notch stress and strain ranges and $\Delta S, \Delta e$ are nominal stress and strain ranges respectively. Equation (4) may be rewritten as

$$(\Delta\sigma \Delta\epsilon E)^{1/2} = K_f \Delta S \tag{5}$$

to relate the local and nominal stress and strain behavior. Note that $\Delta\sigma$ and $\Delta\epsilon$ are also related through the cyclic stress-strain curve eq. (1). According to Petersen [6] K_f is related to the notch geometry by

$$K_f = 1 + q(K_t - 1) \tag{6}$$

where K_t is the theoretical elastic stress concentration factor, a function of detail geometry, and q is the notch sensitivity coefficient defined by

$$q = \frac{1}{1 + (\phi/\rho)^\kappa} \tag{7}$$

In eq. (7), ρ is notch root radius and κ and ϕ are material-dependent constants.

The determination of q and K_f traditionally has been one of the problem areas in analytical studies of low-cycle fatigue at notches. In high-cycle fatigue, where the notch behavior is essentially elastic, $K_f \approx K_t$. In low-cycle fatigue, however, it has been consistently observed that the reduction in fatigue strength shown by notch compared to smooth specimens is not as great as would be anticipated from K_t, i.e. $K_f < K_t$. Raske [7] suggests this to be due to strain gradient or size effects, although recent studies by Leis, et al [8] indicate that it is more likely due to progressive changes in K_f relative to K_t (eq. (5)). In any event, there is little doubt that some semi-empirical approach is needed in order to define K_f.

Although Serensen [9] and others have shown that K_f varies somewhat over the spectrum of fatigue lives, it is a reasonable and simplifying assumption that K_f is constant over a limited range of lives [27]. Moreover, in view of the unquestionably material dependent nature of q, it seems desirable to determine the appropriate constants ϕ and κ in eq. (6) by regression analysis of data obtained from the specific material of interest. Specifically, with a controlled notch (geometry known) and an appropriate nominal and notch instrumentation K_σ and K_ϵ may be found from measured nominal and notch strains and the cyclic stress-strain curve; hence K_f from eq. (4). With K_t known, q may be calculated from eq. (6). Finally, a regression analysis of q on κ is performed, from which ϕ and q are obtained. For steels with yield strengths of around 100 ksi values of $\phi = 0.125$ and $\kappa = 0.75$ appear to be representative, when the notch root radius $\rho < 0.10"$.

The theoretical elastic stress concentration factor K_t is a function of the detail geometry, and is the primary mechanism for relating the highly localized material response at cracking sites in large scale structural information. In the case of highly complex details, K_t can be calculated by specialized finite-element methods. Twelve noded isoparametric elements are used as described in reference [10]. Because of their ability to model high strain gradients and the reduction of computer costs (due to savings in data preparation and turn-around time) in all stress concentration problems the isoparametric elements are much to be preferred to the conventional constant strain elements. Sensitivity studies for butt and fillet welds showing the effects of weld geometry on stress concentration and stress intensity can now be obtained using finite element methods. Although the results discussed in this paper will deal only with the elastic analysis, work is underway [10] to extend the analysis into inelastic range. This will lead to a better appreciation of the limitations of the Neuber's rule discussed earlier and also permit the application of elastic-plastic fracture mechanics concepts.

2.4 Computer Simulation of Notch Response

With the information on basic material response and a stress analysis relating nominal and local stress-strain behavior, crack initiation can be predicted by the computer simulation of the local stress-strain response to structural loading. This is illustrated conceptually in Figure (2). The non-zero starting point for the notch reflects the presence of an initial residual stress. The hysteresis trace is obtained by scaling eq. (1) and the control conditions for each stress-strain reversal are provided by eq. (5). Transient cyclic response which accounts for the gradual change from monotonic to stabilized cyclic strain curve can also be simulated. A variant of the Miner's rule [11] suggested by Wetzel [12] is used. Here, damage accumulation is added cycle by cycle in conjunction with eq. (2) and notch simulation to predict crack initiation under variable amplitude conditions.

3. Crack Propagation Analysis

3.1 General Considerations

Fracture mechanics concepts are used to study the growth of fatigue cracks. For the design application one might assume that the crack growth begins from the very first load cycle or that it follows crack initiation phase discussed above. In the first case the initial crack would correspond to the maximum depth that could conceivably be missed by non-destructive inspection methods. In the second case the initial crack could correspond to the size at the end of the initiation phase which we have defined roughly as a semi-elliptical flaw of 3/16" surface length and a depth of 1/16". Considering or neglecting the initiation phase provides an estimate of upper or lower bound of the fatigue performance. For the purpose of simplicity in the analysis and in the direction of design conservativeness an edge crack (a/2c ratio of zero) will be assumed.

In the following we shall assume that linear elastic fracture mechanics is applicable for the characterization of growth rates, even for the cases where the applied stress range approaches uniaxial yield stress. This assumption appears reasonable in view of Rice's [13] suggestion that the cyclic plastic zones are roughly one-quarter of the plastic zones incurred under monotonic loading.

Analogous to the procedure described in Figure 1 for crack initiation analysis the basic elements of crack propagation analysis are: (a) material characterization data which yields crack propagation law, (b) stress analysis for stress intensity factor at complex structural details, and (c) synthesis of (a) and (b) expressed as the curve of crack depth a versus the number of cycles N required to propagate the crack from an initial size a_o to the final crack size a_f. These elements will be discussed individually. Attention shall be focused on flaws growing from the surface; it may be expected that for pressure vessels operating at low cyclic frequencies in a corrosive environment the growth of external flaws will normally be the controlling factor in the design.

3.2 Crack Propagation Law

The simplest form of the relation between the crack size a and cycles N is specified in terms of the growth rate expression suggested by Paris [14]

$$\frac{da}{dN} = C_P(\Delta K_I)^{\beta} \quad ; \Delta K_I = (K_I)_{MAX} - (K_I)_{MIN} \tag{8}$$

Here, K_I is the fracture mechanics stress intensity factor range, (K_I) max and (K_I) min are respectively the maximum and minimum stress intensity factors of the cycle and C and β are regression constants determined from crack growth rate tests of small specimens. The constant C_P depends on the mean cycling stress. It might be emphasized that the growth relation should be generated at cyclic frequencies and an environment similar to the anticipated service condition. The constant β has been observed to be largely independent of the mean stress. Possibly on account of initial residual compressive stresses crack growth rates for weldments generally have been observed [15-16] to be lower than for base material so that the use of base material characterization data should be in the direction of design conservativeness.

3.3 Stress Intensity Factor Calculations

The stress intensity factor depends on the crack size, structural geometry and applied stress and may be expressed in general form as

$$K_I = F(a/W) S \sqrt{\pi a} \tag{9}$$

Here, $F(\frac{a}{W})$ is a finite geometry correction factor and for the edge cracks under consideration is a function of a/W, the ratio of crack size a to the thickness of the plate W.

Although closed form K_I solutions for applied tension or bending are available [17] in the technical literature a special problem may arise in their application to structural weldments. As pointed out by Lawrence [18] the cracks emanating from the geometric notches resulting from the toes of fillet or butt welds are subjected at least initially to highly nonlinear stress gradients. An additional source of gradients may be the initial residual stresses, or stresses due to thermal fluctuations. In such cases the degree of accuracy of standard solutions is uncertain and recourse must be made to specialized methods of analysis.

One such method is based on the application of finite element techniques. Singular crack tip core elements are combined [10] with the isoparametric elements discussed earlier in connection with the stress concentration problem. K_I solution is obtained directly from the computer output. The only disadvantage of this method is that for the purpose of crack propagation analysis K_I is required as a continuous function of crack depth. This means that finite element idealization must be performed for a large number of crack depth increments and the results curve fitted by a polynomial function.

The second method although more approximate requires only: (a) the knowledge of normal stress distribution along the plane to be traversed by the crack, (b) closed form solution (Green's function) for a concentrated load acting at any point on the crack surface. The central idea here is that of elastic superposition; only the stresses relieved by crack advance contribute to the K_I calculation. The essentials of the method are described in reference [18], where Emery's solution [19] for an edge crack in a half-plane loaded by an arbitrary stress field was used. In our procedure, a Green's function approach is used to derive the stress intensity solution for a cracked plate of finite width where a trapezoidal pressure distribution is applied between two arbitrary points on the crack surface. Isoparametric finite element analysis is then employed to obtain discrete values of the stresses along the plane to be traversed by the crack in an equivalent uncracked section. Piecewise linearization of this stress distribution enables the total stress intensity factor to be computed as a summation of stress intensity increments, each increment being computed from the Green's function analysis above.

3.3 Integration of Crack Growth Law

The number of cycles Np required to propagate a crack from an initial size a_o to some size a_f may be obtained by integration of eq. (8)

$$N_p = \int_{a_o}^{a_f} \frac{da}{C_p(\Delta K_I)^\beta} \qquad (10)$$

Even for constant amplitude cycling, unless F(a/w) of eq. (9) is a very simple function of crack size, the integration must be performed numerically. For variable amplitude loading the integration is complicated by the possibility of crack retardation effects. However, in the direction of design conservativeness, these effects may be neglected and the integration performed either cycle by cycle or in the same manner as for constant amplitude loading but using the root mean square (rms) value of the cyclic stress fluctuation.

The selections of the "critical" crack size $a = a_f$ terminating the end of the useful fatigue life of the weldment deserves some comment. In weldments for which fracture toughness K_{Ic} (or $K_{I scc}$ appropriate to corrosive environment) can be measured, the critical crack size a_f can be calculated by setting $K_I = K_{Ic}$ in eq. (9). The stress S would be the maximum total tensile stress of the cycle and should reflect the contribution of initial residual tensile stress. For small flaws plasticity correction should be included. However, for tough materials the calculation of a_f in the above manner may allow crack sizes approaching the thickness of the plate which may be unacceptable from the standpoint of excessive deflections. In such a case an arbitrary but more pragmatic approach in defining "failure" may be used. For example, a_f may be selected as corresponding to ΔK_I on $\frac{da}{dN}$ vs ΔK_I material characterization curve for which the crack growth rates become fairly large (say 10^{-3} inch/cycle). Alternatively, as in reference [18], a_f may be selected as an arbitrarily small percentage of the plate thickness.

4.0 Probabilistic Reliability Analysis

4.1 General Considerations

The fundamental concept underlying the probabilistic approach to structural reliability is that of risk or probability of failure. When the forcing functions S_F and structural capacity R are statistically independent random variables with known probabilistic description, the probability of failure is [20]

$$P_f = P_r\left[R < S_F\right] = \int_0^\infty F_R(S) f_S(S)\, dS \qquad (11)$$

in which $F_R(S)$ and $f_S(S)$ denote distribution and density function, respectively, of R and S_F.

The probabilistic descriptions of R and S_F relevant to evaluating structural reliability are seldom known in practice [21]. Although their means and variances may be available, their behavior at the extremes of the probability distributions, which is the region significant for computing structural risk, would probably remain undetermined, even if additional data were acquired. Probability distributions for R and S_F therefore must usually be selected by physical argument or for convenience. This is not a serious shortcoming, however, provided that the risks thus obtained are interpreted in a comparative sense [22] and that the reliability model is used consistently throughout the safety analysis.

Since the random variable R (or S_F) of eq. (11) is usually a function of other random variables, i.e. $R = g(y_1, y_2 \cdots y_n)$, its mean and variance may be determined approximately in terms of means and variances of component variables by expanding R in a Taylor series about the means, linearizing, and taking moments of the result. This yields [23]

$$\bar{R} \approx g(\bar{Y}_1, \bar{Y}_2 \dots \bar{Y}_n)$$

$$\sigma_R^2 \approx \sum_{i=1}^{n} \left(\frac{\partial g}{\partial Y_i}\right)^2 \sigma_{Y_i}^2 + 2\sum_{i=1}^{n-1} \sum_{j=i+1}^{n} \left(\frac{\partial g}{\partial Y_i}\right)\left(\frac{\partial g}{\partial Y_j}\right) r_{ij}\, \sigma_{Y_i} \sigma_{Y_j} \tag{12}$$

in which the bar over a variable denotes its mean value, σ_R is variance of R and r_{ij} is the correlation coefficient between Y_i and Y_j. If all Y's are mutually statistically independent, $r_{ij} = 0$. The coefficient of variation (c.o.v) $\Omega_R = \sigma_R/\sqrt{R}$ is an appropriate measure of statistical uncertainty. In practice, it may be obtained [20] as $\Omega_R = \sqrt{\delta_r^2 + \Delta r^2}$, in which δ_R is data-based basic randomness or variability and Δr is the prediction error arising from insufficient information, relying in part on subjective engineering judgment. This approach thus provides a mechanism for incorporating engineering judgment in the reliability analysis; it is not desirable that the capability for incorporating engineering judgment and experience be entirely removed.

A detailed discussion of probabilistic analysis of crack growth is contained in reference [24]. A summary of the initiation analysis [25] is presented in the following.

4.2 Application to Crack Initiation Analysis

The probability distribution for crack initiation period N_i is well represented by the Weibull distribution [20]

$$P_r[N_i \le n] = F_{N_i}(n) = 1 - \exp\left[\left(\frac{n}{\mu}\right)^{\alpha}\right] \tag{13}$$

in which α and μ are related to the mean and c.o.v. of N_i by

$$E[N_i] = \mu\, \Gamma(1 + 1/\alpha) \tag{14}$$

$$\Omega_{N_i}^2 = \frac{\Gamma(1 + 2/\alpha)}{\Gamma^2(1 + 1/\alpha)} - 1 \tag{15}$$

where E $[N_i]$ denotes the mean and Γ is the gamma function.

The mean and c.o.v. of N_i determined from the regression analysis of eq. (2) are conditional, since they imply that $\Delta\epsilon$ is known. Since the weld geometry, applied and residual stresses are actually random variables in practice, the notch strain, which is required to predict crack initiation in the structural weld, is also random. Therefore the statistical variability of $\Delta\epsilon$ will also contribute to the overall variability in N_i for a structural weld. The unconditional mean of N_i is [26]

$$E[N_i] = E[E(N_i/\Delta\epsilon)] \tag{16a}$$

If the variability of $\Delta\epsilon$ is not too large, we may assume that $E[E(N_i/\Delta\epsilon)] = E[N_i/\Delta\bar{\epsilon}]$ where $E[N_i/\Delta\bar{\epsilon}]$ is obtained from eq. (2). The unconditional variance of N is [26]

$$Var(N_i) = E[Var(N_i/\Delta\epsilon)] + Var[E(N_i/\Delta\epsilon)] \tag{16b}$$

The first term is the "average" variance of N_i when $\Delta\epsilon$ is known, which is found from the scatter about the $\Delta\epsilon$ *vs.* N_i baseline data shown schematically in Figure 2. The second term is the contribution of additional variance to N_i from statistical variations in $\Delta\epsilon$ that arise as a result of variabilities in notch geometry and residual stress. Using eq. (12) and noting that Ω_m is very small for a given class of steels, the uncertainty in N_i is

$$\Omega_{N_i}^2 = \delta_{N_i}^2 + \frac{1}{m^2}\Omega_{\Delta\epsilon}^2 \tag{17}$$

where δ_{N_i} as well as m are evaluated from the baseline data (represented by eq. (2)) and $\Omega_{\Delta\epsilon}$ is uncertainty in notch strain range. The Weibull shape factor α_N can then be determined from eq. (15). Note that eq. (17) enables the variability in fatigue performance of a structural weld to be evaluated in terms of uncertainties in small specimen fatigue test data and variabilities in weld geometry. The notch strain would be a function of K_f, ΔS, and residual stress. Consistent with the first-order approach, its mean $\Delta\bar{\epsilon}$ is found from the deterministic crack initiation analysis discussed above. Its uncertainty, assuming stress and strain to be perfectly correlated through the stress-strain curve, may be shown to be (approximately)

$$\Omega_{\Delta\epsilon}^2 \approx \frac{1}{2}\left[4(\Omega_{K_f}^2 + \Omega_{\Delta S}^2) + \Omega_{\sigma_n\,max}^2\right] + \Delta^2 e_g \tag{18a}$$

in which Ω_{K_f}, $\Omega_{\Delta S}$ and $\Omega_{\sigma_n\,max}$ are uncertainties in K_f, ΔS, and maximum notch (residual) stress and Δe_g represents the prediction error in the analysis used to determine $\Delta\epsilon$. The uncertainty in K_f may be further broken down according to eq. (5) and (12)

$$\Omega^2_{K_f} = \left(q \frac{K_t}{K_f} \right)^2 \delta^2_{K_t} + \left(K_f - 1 \right)^2 \Delta^2_q \qquad (18b)$$

where δ_{K_t} would represent data-based variability in the notch geometry and Δ_q the prediction error in determining q.

The probability of initiating fatigue cracks during the design life N_D can be found from eq. (13). Conversely, a cycling stress level can be chosen so that the risk $P_D = P_r(N_i \leq N_D)$ of initiating cracks in N_D is acceptably small. Specifically, given C and m of eq.((2) and α_{N},

$$\Delta\epsilon(P_D) = C\left[\frac{1}{N_D} \log\left(\frac{1}{1-P_D} \right)^{1/\alpha_N} \right]^m \qquad (19)$$

Although the above analysis is applicable to the case of a single crack the probability of a number of cracks during the specified design life can also be calculated [25]. This permits the design estimate of the "size" effect i.e. the dependence of the initiation probability on the length of the weld.

5.0 Illustrative Example

Figure 3 shows an untreated butt weld for which predictions are to be made for crack initiation and growth under constant amplitude cycling. Parameters which describe the geometry of the weld are shown in Figure 3a. The weld contains a stress raiser in the form of an undercut of depth a_u and root radius ρ. Crack growth is assumed in the direction of plate thickness leading to crack depth a_f measured from the top of the plate.

Figure 3b shows finite element idealization for W = 1.0 in., a_o = 0.025 in., T_w =1.154 in, $\theta = 30°$, and ρ = 0.005 in. For the case of remote axial tensile stresses to obtain the stresses, only one quadrant of the joint is idealized. The analysis is first performed to obtain the stress distribution for the original undercut geometry. For this purpose 22 elements and 141 nodes are used. Stress intensity factors K_I calculations for cracks originating from the weld undercut require a circular core tip element and a total of 26 elements and 170 nodes.

Figure 3c shows the normal stress distribution (in S - direction) inward from the toe of the weld. The stresses are normalized with respect to the applied stress indicating stress concentration K_t = 7.49 at the toe of the weld.

Figure 3d shows the comparison of stress intensity calculations for cracks emanating from the notch for a unit applied stress (S = 1 ksi) using three methods. The first is based on the finite element idealizations and is considered to be most accurate at least for very small flaws in the root of the notch. The second is the K_I analysis for a semi-elliptical surface flaw in flat plate under tension proposed by Shah and Kobayashi [27] and assume that a/2c ratio=0. The solution takes into account finite thickness of the plate. The third is based on the formula $K_I = 1.12 S\sqrt{\pi a}$, which is considered to be valid only for shallow two dimensional edge cracks [17]. The results appear to be essentially the same except for very small flaws, where the finite element method which considers stress concentration effect of the initial notch indicates higher values.

Figure 4 contains the results of crack initiation and growth computations for 80 ksi yield strength weld idealized in Figure 3. For K_t = 7.49 obtained from the finite element analysis and the material notch sensitivity parameters ϕ = 0.0125, λ = 0.75, q and K_f of 0.335 and 3.17 are obtained respectively from eq. (7) and eq. (6). The notch simulation analysis for specified ΔS is started assuming a initial residual tensile stress of 40 ksi. Because of the high stress concentration,yielding will occur at the notch after the first excursion, even for small values of ΔS. Thereafter the mean stress will relax toward zero and the notch stress-strain hysteresis will approach one of fully reversed stress with $\sigma_{max} = -\sigma_{min}$ = 80 ksi. For any K_f and ΔS, the notch strain range $\Delta\epsilon$ can be calculated from the stabilized cyclic stress strain curve (eq. 1) in accordance with the scheme of Figure 2. For example with ΔS = 46 ksi and K_f = 3.17, $\Delta\epsilon$ = 0.0058 and N_i = 20,350 cycles. It should be noted that $\Delta\epsilon$ and hence N_i are calculated for a fixed product $K_f \Delta S$. This permits design sensitivity comparisons between a severe stress concentration (high K_f) and low ΔS or high ΔS and a mild stress concentration (low K_f) which could be achieved by appropriate weld treatment.

Crack propagation analysis is carried out using $C_p = 1.5 \times 10^{-9}$ and β = 2.5 from Barsom's data [28] for 80 ksi yield strength material in air environment. Numerical integration of eq. (10) uses the Shah and Kobayashi formula for K_I; since the formula underpredicts K_I for very small cracks emanating from the notch the crack propagation results are likely to be somewhat unconservative. Improvement in the analysis could be expected by using a polynomial function representation of the finite element K_I calculation. Figure 4a shows the curves of crack depth a vs number of propagation cycles N_p for two initial flaws a_o. The first corresponds to $a_o = a_{Ni}$; the undercut is treated as a sharp crack. The second corresponds to the initial depth of $a_0 = a_{N_i} + 0.0875"$; the fatigue crack propagation is assumed to commence after N_i cycles required to initiate the crack from the weld undercut. For both cases it is assumed quite arbitrarily, that the "failure" $N = N_p$ occurs when the crack reaches the depth of 0.325 in. Judging from the rapidly increasing slope of a vs N curve in Figure 4a the useful life remaining for $a > 0.325$ in. can be neglected.

The results from the crack initiation and growth analysis are summarized in Figure 4b where four curves of S vs N are shown, each curve corresponds to a different definition of N. In the first curve $N = N_i$, i.e. crack propagation life is neglected. In the second curve $N = N_i + N_p$ where the number of cycles corresponding to crack initiation is added to the number of cycles required to propagate the crack from an initial depth $a_0 = a_N + 0.0875$ to an assumed "critical" crack of 0.325 in. This is consistent with our definition of crack initiation in baseline which implicitly recognizes some growth from the surface. Ignoring the crack initiation phase entirely leads to $N = N_p$ shown in curve no. 3. An upper bound on fatigue performance is obtained in curve no. 4 which assumes $N = N_i + N_p$. However in contrast with curve no. 2 N_p is defined as in curve no. 3. At the end of the initiation life N_i the depth of the initial crack is assumed to be negligible. As can be seen from this example even for a very sharp notch the duration of the crack initiation phase can be a significant proportion of the total fatigue life.

In the first-order probabilistic assessment of crack initiation, it is assumed that the foregoing deterministic analysis is sufficient to relate the mean values of the various parameters, while the uncertainties and design risk can be computed according to eqs. (17), (18), and (19). It is assumed that the uncertainity in load is $\Omega_{\Delta S} = 0.05$ from past service records. Because notch cycling takes place in the plastic range, $\Omega_{\sigma_{N_{MAX}}} \approx 0.0$, with $\sigma_{MAX} = -\sigma_{MIN} = 80$ ksi. Using eq. (18b) and supposing that $\delta_{K_t} = 0.11$ from notch measurements and $\Delta q \approx 0.025$ (subjectively), $\Omega_{K_f} = 0.10$ and thus $\Omega_{\Delta\epsilon} = 0.18$ from eq. (18a). The uncertainty in the baseline crack initiation data, δ_{N_i} is 0.30, which is computed from the experimental scatter about the regression line given as eq. (2). Eqs. (17) and (15) yield $\Omega_{N_i} = 0.63$ and $\alpha_N = 1.64$. With the parameter α_N determined and with $\Delta\epsilon$ related to ΔS through the deterministic notch simulation analysis described above, eq. (19) can be used to determine the relationship between K_f, ΔS, P_D , and N_D. This relation is illustrated in Figure 4c. Although plotted as P_D vs ΔS to establish correspondence with Figure 4b, curve 1, a general relation between K_f ΔS and P_D can also be established which allows tradeoffs to be made between design risk, structure life, allowable stresses, and weld treatments [25].

6.0 Summary

A comprehensive approach to low cycle fatigue assessment of structural welds based on the utilization of small specimen data and structural analysis is presented. The analysis is based on the prediction of crack initiation, and crack propagation at stress raisers. Finite element methods are used to estimate stress concentration and stress intensity factors at complex weld geometries. Because of the statistical variability inherent in the material characteristics, weld flaw geometry, and the load spectrum, probabilistic analysis is also included.

The methodology presented in this paper will prove useful for the selection of design stress levels, and establishment of weld acceptance standards.

Acknowledgments

The authors are indebted to Mr. Don Martin for the numerical computations.

REFERENCES

[1] Morrow, J., "Cyclic Plastic Strain Energy and Fatigue of Metals," in "Internal Friction, Damping and Cyclic Plasticity" Am. Soc. Testing Mat. STP 378 (1965).
[2] Gross, M.R., "Low Cycle Fatigue of Materials for Submarine Construction," Navy Eng. J. (Aug 1963).
[3] Smith, K.N., Watson, P., Topper, T.H., "A Stress-Strain Function for the Fatigue of Metals," J. Materials JMLSA, Vol 5, No. 4 (Dec 1970).
[4] Neuber, H., "Theory of Stress Concentration for Shear-Strained Prismatical Bodies with Arbitrarily Nonlinear Stress-Strain Law," J. Appl. Mech. ASME, Vol. 83, No. 4 (Dec 1961).
[5] Topper, T.H., R.M. Wetzel, Jo. Dean Morrow, "Neuber's Rule Applied to Fatigue of Notched Specimens," J. Materials, Vol 4, No. 1 (1969).
[6] Peterson, R.E., "Stress Concentration Design Factors," John Wiley and Sons, New York (1953).
[7] Raske, D., "Section and Notch Size Effects in Fatigue," Univ. of Illinois Dept. Theor. and Appl. Mech. T&AM Report 360 (August 1972).
[8] Leis, B.N., Gowda, C.V.B., Topper, T.H., "Cyclic Inelastic Deformation and the Fatigue Notch Factor," in Cyclic Stress-Strain Behavior-Analysis, Experimentation and Failure Prediction," Am. Soc. Testing Materials, Keoto, Japan (Aug 1971).
[9] Serensen, S., Machutov, N., Schneiderovitch, R., "Criteria of Two Types of Low Cycle Nonstationary Fracture of Steel," Proc. International Conference on Mechanical Behavior of Materials, Kyoto, Japan (Aug 1971).
[10] Hilton, P.D., Gifford, L.N., and Lomacky, O., "Finite Element Fracture Mechanics Analysis of Two Dimensional and Axisymmetric Elastic and Elastic-Plastic Cracked Structures," Naval Ship Research and Development Center Report No. 4493, (Nov 1974).
[11] Miner, M.A., "Cumulative Damage in Fatigue," J. Appl. Mech. No. 12, pp 159-164 (1945).
[12] Wetzel, R.M., "A Method of Fatigue Damage Analysis," Ford Motor Company, Metallurgy Res. Report (Sept 1971).
[13] Rice, J.R., "Mechanics of Crack Tip Deformation and Extension by Fatigue," ASTM STP 415, p. 247 (June 1967).
[14] Paris, P.C., "The Fracture Mechanics Approach to Fatigue," in "Fatigue an Interdisciplinary Approach" Syracuse University Press, Syracuse, N.Y. (1964).
[15] Clark, W.J., Jr., Kim, D.S., "Effect of Synthetic Seawater on the Crack Growth Properties of HY-140 Steel Weldments," Engineering Fracture Mechanics, Vol 4, pp 499-510 (1972).
[16] Parry, M., Nordberg, H., Hertzberg, R.W., "Fatigue Crack Propagation in A514 Base Plate and Welded Joints," Lehigh University, Fritz Engineering Laboratory Report 358.33 (Sept 1971).
[17] Tada, M., "Stress Analysis of Cracks Handbook," Del Research Corporation (1973).
[18] Lawrence, F.V., "Estimation of Fatigue-Crack Propagation Life in Butt Welds," Welding Research Supplement, p. 212 (July 1970).
[19] Emery, A.F., Walker, G.E., Jr., "Stress Intensity Factor for Edge Cracks in Rectangular Plates with Arbitrary Loadings," ASME Publication 62-WA/MET-18 presented at ASME Winter Annual Meeting and Energy Systems Exposition, New York (December 1968).
[20] Freudenthal, A.M., Garretts, H.M., Shinozuka, M., "The Analysis of Structural Safety," Journ. Struct. Div. ASCE, Vol. 92, No. ST1, (Feb 1966).
[21] Ellingwood, B.R., Ang, A.H.-S, "Risk-Based Evaluation of Design Criteria," Journ. Struct/ Div. ASME Vol. 100, No. ST9 (Sept 1974).
[22] Bolotin, V.V., "Statistical Methods in Structural Mechanics," Holden-Day, San Francisco, (1969).
[23] Ang, A.H.-S, and Cornell, C.A., "Reliability Bases of Structural Safety and Design," Journ. Struct. Div. ASME., Vol. 100 No. ST9 (Sept 1974).
[24] Lomacky, O., Ang., A.H.-S. and Amin, H., "Fatigue and Fracture Reliability Analysis of Pressure Vessels," First National Congress on Pressure Vessels and Piping, San Francisco, California, Paper 71-PVP-47 (May 1971).
[25] Ellingwood, B.R., "Probabilistic Assessment of Low Cyclic Fatigue Behavior of Structural Welds," Second National Congress on Pressure Vessels and Piping, San Francisco, California (June 1975).
[26] Parzen, E., "Stochastic Processes," Holden-Day, San Francisco (1967).
[27] Shah, R.C., Kobayashi, A.S., "On the Surface Flaw Problem in the Surface Crack: Physical Problems and Computation Solutions," The American Society of Mechanical Engineers (1972).
[28] Barsom, J.M., Imhof, E.J., Rolfe, T.S., "Fatigue Crack Propagation in High Yield-Strength Steels," Eng. Fract. Mech. Vol. 2, pp. 301-317 (1971).

L 6/6

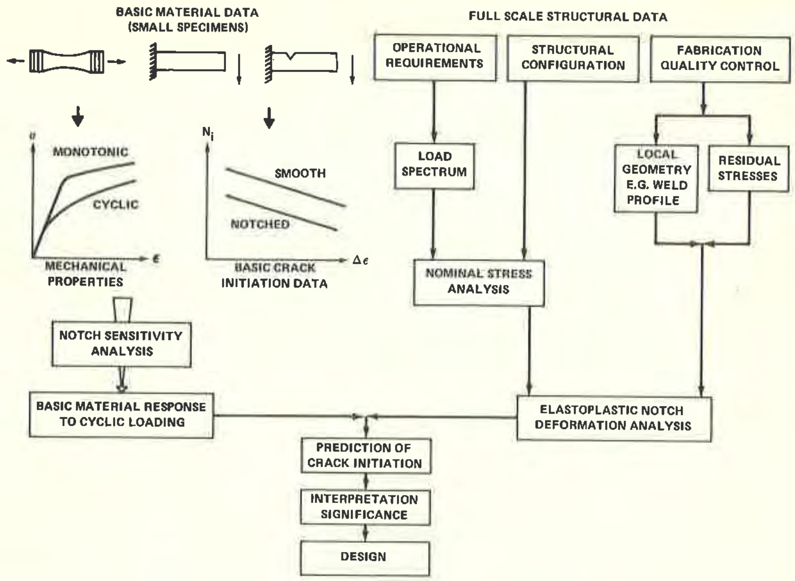

FIG. 1 ESSENTIALS OF CRACK INITIATION ANALYSIS

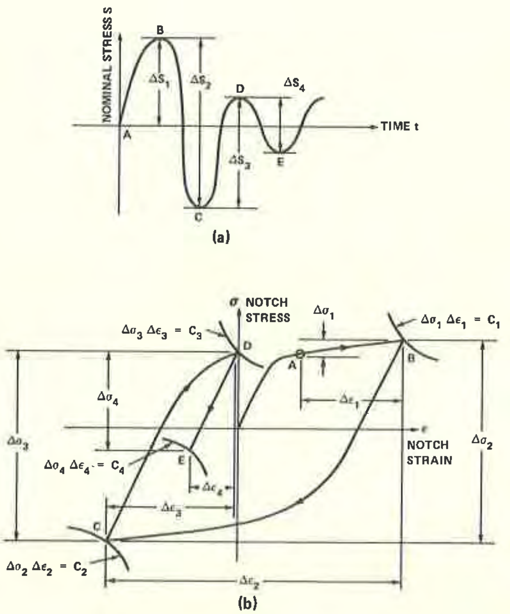

FIG. 2 COMPARISON OF NOMINAL AND LOCAL STRESS-STRAIN HISTORY OF NOTCHED SPECIMENS

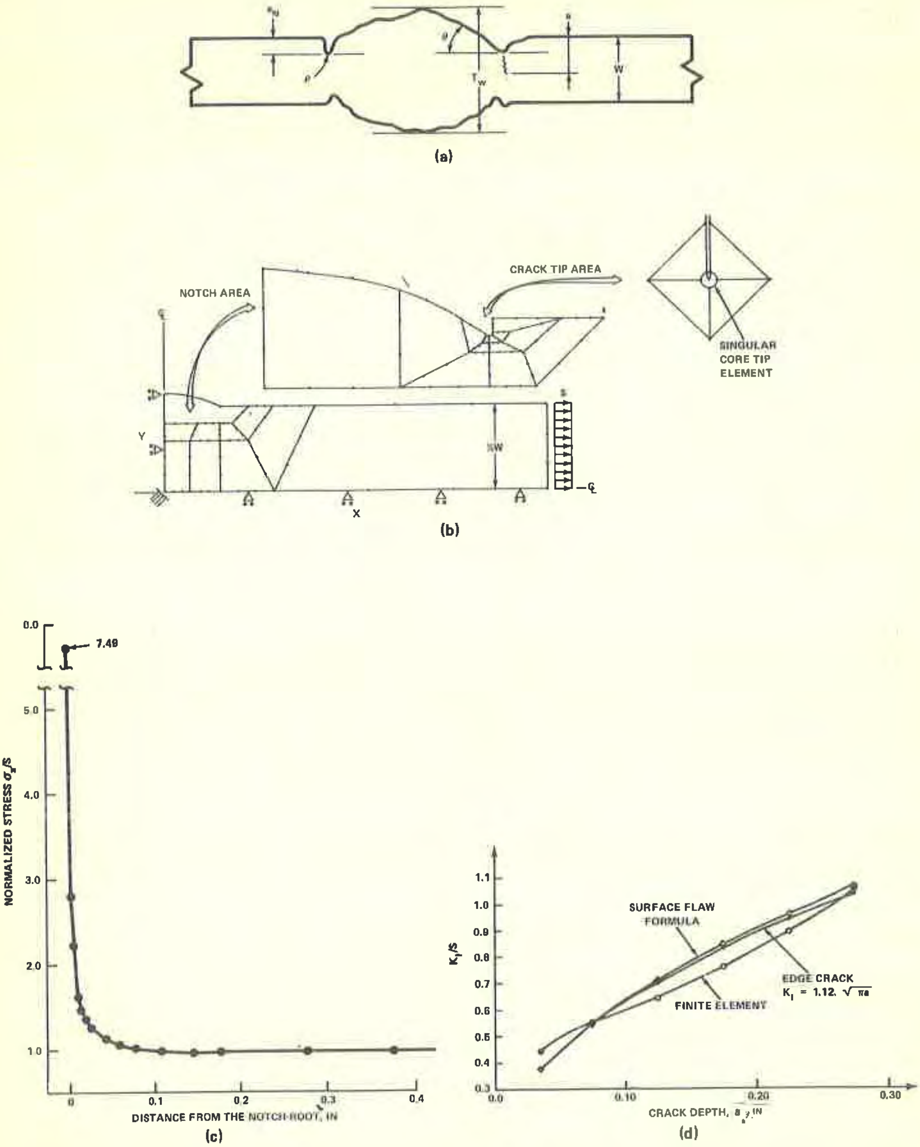

FIG. 3 TYPICAL BUTT WELD

(a) WELD GEOMETRY
(b) FINITE ELEMENT IDEALIZATION FOR T_W = 1.154 IN, $\Theta = 30^0$
a_o = 0.025 IN, ρ = 0.005 IN
(c) STRESS VARIATION INWARD FROM THE WELD UNDERCUT
(d) STRESS INTENSITY FACTOR FOR S = 1 KSI VS CRACK DEPTH

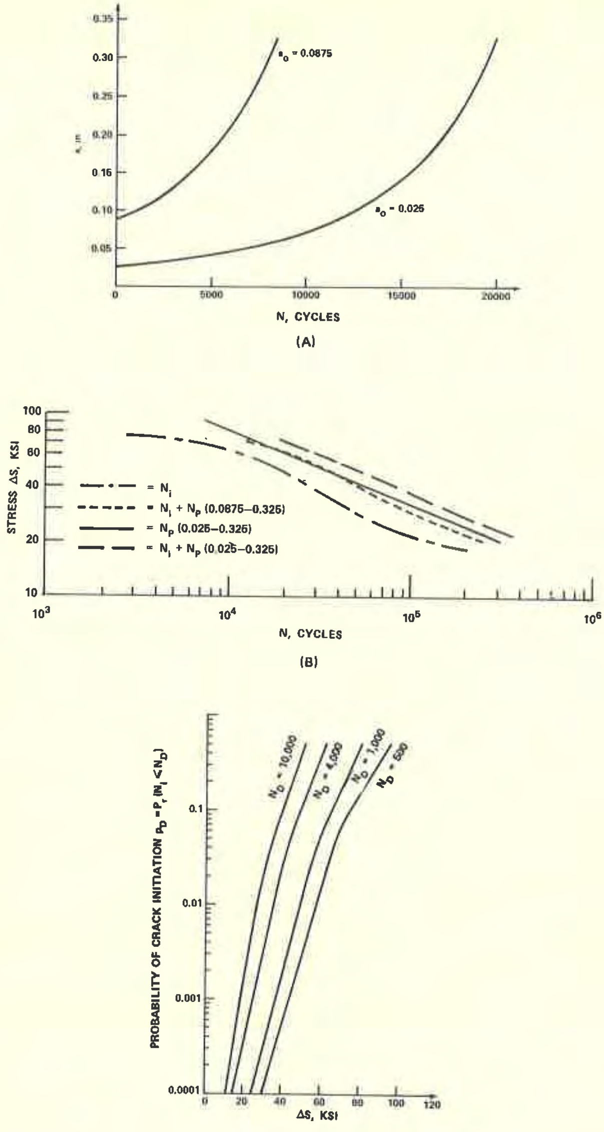

FIG. 4 CRACK INITIATION AND GROWTH CALCULATIONS RESULTS

(A) CRACK DEPTH VS NUMBER OF CYCLES

(B) STRESS RANGE VS NUMBER OF CYCLES TO FAILURE

(C) PROBABILITY OF CRACK INITIATION VS STRESS RANGE